mathematics

MDPI

Article

Optimization of Load Distribution Method for Hydropower Units Based on Output Fluctuation Constraint and Double-Layer Nested Model

Hong Pan [1], Zhengliang Luo [2], Chenyang Hang [1,*], Yuan Zheng [1], Fang Feng [3] and Xiaonan Zheng [1]

[1] College of Energy and Electrical Engineering, Hohai University, Nanjing 211100, China; hongpan@hhu.edu.cn (H.P.); zhengyuan@hhu.edu.cn (Y.Z.); 221306020013@hhu.edu.cn (X.Z.)
[2] Ming Yang Smart Energy Group Limited, Zhongshan 528436, China; luozhengliang@mywind.com.cn
[3] Shanghai Aircraft Design and Research Institute, Shanghai 200135, China; fengfang@comac.cc
* Correspondence: 211606010028@hhu.edu.cn

Abstract: During the load distribution of hydropower units, the frequent crossing of vibration zones as well as large output fluctuations affect the stability of the power station. A multi-objective double-layer intelligent nesting model that considers the constraint of the output fluctuation of units is proposed to address these problems. The nonlinear constraint unit commitment optimization model layer is built based on outer dynamic programming, and the load distribution optimization model layer is constructed based on the improved biogeography-based optimization algorithm. Simultaneously, the unit output fluctuation constraint is established based on whether the unit combination changes in order to limit the unit output fluctuation. The results of this model indicate that compared with traditional load allocation models, the application of the method proposed in this paper can reduce the fluctuation range of unit output by 85.01%. In addition, except for the inevitable vibration zone crossings during startup and shutdown processes, the unit does not cross the vibration zone during operation, which greatly improves the unit's vibration isolation and optimization capabilities. The multi-objective double-layer intelligent nested model proposed in this paper has significant advantages in the field of load allocation for hydropower units. It effectively improves the stability and reliability of unit operation, and this method can be applied to practical load allocation processes. It is of great significance for the research on load allocation optimization of hydropower units.

Keywords: unit output fluctuation; double-layer nested model; improved biogeography-based optimization algorithm; load distribution optimization; hydropower unit; crossing vibration zone

MSC: 90-10

check for updates

Citation: Pan, H.; Luo, Z.; Hang, C.; Zheng, Y.; Feng, F.; Zheng, X. Optimization of Load Distribution Method for Hydropower Units Based on Output Fluctuation Constraint and Double-Layer Nested Model. *Mathematics* **2024**, *12*, 662. https://doi.org/10.3390/math12050662

Academic Editors: David Barilla, Nicu Bizon and Alessandro Niccolai

Received: 4 January 2024
Revised: 5 February 2024
Accepted: 22 February 2024
Published: 24 February 2024

Copyright: © 2024 by the authors. Licensee MDPI, Basel, Switzerland. This article is an open access article distributed under the terms and conditions of the Creative Commons Attribution (CC BY) license (https://creativecommons.org/licenses/by/4.0/).

1. Introduction

During the operation of hydropower units, the power station needs to coordinate the startup/shutdown and output between units and complete its load distribution according to the optimization goal of "the maximum benefit of the power station" or "the minimum water consumption of the power station" [1]. Moreover, some nonlinear and nonconcave constraints, including flow constraint, startup and shutdown times, and minimum running time, must be considered to meet the load deviation of the power grid [2]. However, during the actual operation of hydropower units, the received demand load, within a short time, exhibits a large fluctuation range and a corresponding long fluctuation period [3]. Thus, the unit inevitably crosses the vibration zone, which will increase the instability of the unit in the operation process [4]. The traditional dynamic programming model fails to perform a reasonable and efficient load distribution of the unit at the time and space scale while considering multiple constraints simultaneously. In addition, it cannot account for

the economy and safety of the unit [5], leading to the frequent startup and shutdown of the unit as well as the crossing of the unit through the vibration zone. This reduces the operating life of the unit and affects the stability of the power station [6]. At the same time, with the higher frequency and magnitude of load fluctuations caused by the large-scale grid connection of new energy sources [7], hydropower units need to be able to optimize load distribution even more. In this context, the study of load distribution optimization of hydropower units is particularly crucial [8].

Several studies have attempted to solve the problem of a unit that crosses the vibration zone during operation to realize the safe operation of the unit. Yang et al. [9] proposed an active vibration avoidance control strategy and an active ride-through control strategy. When a hydroelectric unit operates within the vibration zone, the active vibration avoidance control strategy can delay the time for the participating unit to pass through the vibration zone, while the active ride-through control strategy can actively pull up or down the power reference value outside the vibration zone, preventing the unit from operating in the vibration zone. In addition, Wang et al. [10] conducted a joint evaluation by combining economic operating conditions with unit state operating conditions, strictly prohibiting the unit from operating in vibration and vortex zones, in order to achieve maximum power generation efficiency. In the above research, a scheme to limit the operation of the unit in the vibration zone was proposed to reduce the loss. However, it did not fully consider the fluctuation of the unit when crossing the vibration zone and the losses caused by startup and shutdown. In the literature [11,12], the irregular vibration zone constraint was transformed into mixed-integer linear programming (MILP) linear constraint form by adopting a convex subdivision algorithm for the vibration zone, and the unit was optimized by combining the solver. Liao et al. [13] established the MILP model and proposed an iterative direct solution method based on the total head, which not only considers the head change and the water consumption during unit startup and shutdown, but also considers the water consumption crossing the vibration zone. MILP has a wide range of application areas and its modeling is relatively simple. However, MILP has poor scalability, long solving time, limited handling of discrete variables, and limited handling of nonlinear constraints. These drawbacks limit its application in large-scale problems.

Recently, the biogeography-based optimization (BBO) algorithm has been widely used in systems engineering, which requires rapid decision making, because of its advantages, including few adjustable parameters, fast convergence, and good compatibility. Chen et al. [14] improved the transfer model and transfer operator to solve the operational problem under wind power grid connection, thereby achieving approximation of the Pareto optimal frontier solution. Li et al. [15] proposed an adaptive migration rate and added differential perturbations to the migration operator of the migration mechanism, using this improved biogeographical optimization algorithm to optimize the utilization of renewable energy. Liu et al. [16] proposed an updated method for node information exchange in a BBO algorithm based on the small-world characteristics of power grid topology, which reduces the time complexity of the algorithm and improves the efficiency of analyzing complex power grids. Pei et al. [17] employed the migration distance to enhance the migration operator, improve the local search capability, and accomplish the proportional integral derivative (PID) parameter optimization of the controller. Garg et al. [18] applied a constrained Laplacian BBO algorithm to the Economic Load Allocation (ELD) problem in electrical engineering, effectively reducing fuel consumption and emission costs while meeting load demands. However, in the above references, the relationship between individual fitness and population average fitness is not considered to update the migration model and migration operator dynamically in real time. Meanwhile, in the application of BBO algorithms, there is also less research on the field of load distribution of hydropower units under complex and nonlinear constraint conditions.

Based on the aforementioned discussion, a double-layer nested model of improved biogeography-based optimization–dynamic programming (IBBO-DP) with multiple objectives and constraints is developed in this study. First, a daily load distribution model of hydropower units with the objective function of minimizing water consumption was established. Second, the concepts of the unit joint vibration zone and cross-vibration zone risk coefficient, as introduced in [19], were utilized to set vibration zone constraints and unit start–stop constraints, respectively, in order to avoid unit losses caused by crossing vibration zones and frequent start–stop operations. They were also set as penalty terms for the objective function in the program. The inner-layer model was employed for load distribution optimization. Subsequently, the IBBO algorithm was utilized to dynamically adjust the model's migration function based on the relationship between population and individual fitness, and the idea of mixed crossover was introduced in the migration operator to achieve an adaptive update strategy, accelerate the algorithm's convergence speed and optimization ability, and achieve the optimal load distribution for unit combinations. In addition, to reduce the fluctuation in output caused by demand load and combination changes, a constraint for output fluctuation was constructed, and an evaluation index for output variation was established. This index, based on the optimal output distribution in the previous time period, measures and limits the fluctuation in output by judging whether the unit combination has changed. Finally, example calculations demonstrate that compared with the traditional BBO algorithm, this model can effectively improve the convergence speed and accuracy of the algorithm. Furthermore, compared with traditional double-layer dynamic programming, this model can effectively save water consumption, allocate unit loads more reasonably, reduce the number of crossings in unit vibration zones, and decrease the fluctuation in unit output.

2. Daily Load Distribution Model of Hydropower Units

2.1. Objective Function

In this article, the objective function is to minimize the water consumption of the unit, and the calculation method is as follows:

(1) First, the mapping relationship between the flow and efficiency of the turbine is obtained by drawing the comprehensive characteristic curve of the turbine;
(2) After obtaining the historical data of the real hydropower station, data preprocessing and flow evaluation are conducted for the subsequent calculation through data screening, so as to obtain the calculation range of efficiency (since this part is not the core content of this article, it is not described in detail considering the length of the article);
(3) After the unit output is obtained by applying the proposed method to load distribution, the corresponding unit flow is calculated according to the formula $P = 9.81QH\eta$, so as to screen the optimal solution.

(1) The minimum water consumption is expressed as

$$W = min \sum_{i=1}^{I} \sum_{t=1}^{T} \left(Q_{i,t}(H_t, P_{i,t}) * \Delta t + \lambda_{i,t}(1 - \lambda_{i,t-1}) * W_{on_off} + n_{cross} * W_{cross} \right) \quad (1)$$

(2) The minimum deviation from the power grid load is given by

$$\theta_t = min \frac{\left| P_{dt} - \sum_{i=1}^{I} P_{i,t} \right|}{P_{dt}}. \quad (2)$$

In Equations (1) and (2), I is the number of units, T is the number of periods, $Q_{i,t}(H_t, P_{i,t})$ is the flow consumption of the ith unit in period t based on its head and output, Δt is the time granularity, $\lambda_{i,t}$ is the startup/shutdown state of the i-th unit in period t expressed in the binary system with 1 as the starting point and 0 as the stopping point, n_{cross} is the number of times the unit crosses the vibration zone, and W_{on_off} and W_{cross} are the extra startup and shutdown times (excluding the initial startup/shutdown)

of the unit in the dispatching process and the equivalent water loss through the vibration zone, respectively. $P_{i,t}$ and P_{dt} are the output of the ith unit and the demand load of the power grid during period t, respectively, and θ_t is the percentage deviation between the sum of the output of each unit and the demand load of the power grid during period t.

2.2. Nonlinear Constraint Conditions

2.2.1. Basic Constraint Conditions

Simultaneously, other constraints aside from flow, storage capacity, and maximum and minimum output constraints should be considered.

(1) The upper and lower limit constraints of the output are expressed as

$$\left(P_{i,t} - \overline{P_{i,t}}\right)\left(P_{i,t} - \underline{P_{i,t}}\right) \geq 0. \tag{3}$$

(2) The unit startup/shutdown time constraints are as follows:

$$\begin{cases} T_i^{on} - T_{min}^{on} \geq 0 \\ T_i^{off} - T_{min}^{off} \geq 0. \end{cases} \tag{4}$$

(3) The unit additional startup and shutdown time constraints are given by

$$0 \leq \sum_{t=1}^{T} \sum_{i=1}^{I} N_{i,t}^{on,off} \leq N_{max}^{on,off}. \tag{5}$$

(4) The grid demand–load deviation constraint is expressed as

$$P_{dt} * (1 - \delta) \leq \sum_{i=1}^{I} P_{i,t} \leq P_{dt} * (1 + \delta). \tag{6}$$

(5) The water balance and reservoir capacity constraints are expressed as follows:

$$\begin{cases} V_{t+1} = V_t + \left(Q_t^{in} - Q_t^{out}\right) \times \Delta t + Wq_{t-1} \\ V^{min} \leq V \leq V^{max} \end{cases} \tag{7}$$

In the above-mentioned equations, $\overline{P_{i,t}}$ and $\underline{P_{i,t}}$ are the upper and lower limits of the vibration zone in MW, respectively, T_i^{on} and T_i^{off} are the continuous starting and stopping times of the ith unit, respectively, T_{min}^{on} and T_{min}^{off} are the minimum limit times for starting and stopping the i-th station, respectively, $N_{i,t}^{on,off}$ represents the extra startup/shutdown times of the i-th unit at t moment, $N_{max}^{on,off}$ is the sum of the maximum allowable startup/shutdown times of all units in the entire dispatching process, and δ is the deviation of the power grid demand load when the hydropower unit of the hydropower plant is integrated into the grid, which is the initial given parameter of the power plant. V_t, V_{t+1}, V^{min}, and V^{max} represent the storage capacity of the power station at time t and $t + 1$, respectively, and the minimum and maximum values of the storage capacity of the power station, Q_t^{in} and Q_t^{out} represent the inlet flow and outlet flow of the power station at time t, respectively, and Wq_{t-1} represents the disposal volume of the power station at time $t - 1$.

2.2.2. Output Fluctuation Constraint

In the optimal load distribution, the constraint of the unit output fluctuation is added as Z_{t1}, Z_{t2}, …, Z_{tn}, which represents the N unit combinations in period T ($t > 1$), and Z_{t-1}, which is the corresponding combination of optimal load distribution in period $t - 1$, to avoid large fluctuations in the unit output when the demand load fluctuates in a small range in a continuous period.

For any solution Z_{ti} of N combination solutions, the following applies:

(1) If $Z_{ti} \neq Z_{t-1}$, the unit combination changes during the current period. The output $P^*_{i,t}$ of the newly started unit should satisfy the constraint presented in Equation (8) to reduce the fluctuation in the unit output when the combination changes.

$$P^n_{i,min} \leq P^*_{i,t} \leq P^n_{i,max}, \tag{8}$$

where $P^n_{i,min}$ and $P^n_{i,max}$ are the minimum and maximum boundaries of the nth operational zone of the i-th unit, respectively.

Then, the sums of the output of newly started units are added and subtracted, the sum of the output is lost during shutdown, and the change value of the demand load under Z_{ti} combination is obtained, indicating the corresponding output of the continuously started units that needs to be increased or decreased. This is taken as a range constraint to limit its fluctuation.

$$\Delta P = \sum_{i=1}^{I1} P^*_{i,t} - \sum_{i=1}^{I2} P^*_{i,t-1} - \left(\sum_{i=1}^{I} P_{i,t-1} - P_t\right) \tag{9}$$

$$max\left(\sum_{i=1}^{I_{on}} P^{on}_{i,t-1} - \Delta P, P^n_{i,min}\right) \leq P^{on}_{i,t} \leq min(\sum_{i=1}^{I_{on}} P^{on}_{i,t-1} + \Delta P, P^n_{i,min}) \tag{10}$$

Here, $\sum_{i=1}^{I1} P^*_{i,t}$ is the sum of the output of $I1$ newly opened units at time t. This will be 0 if there is no newly opened unit at the current time. $\sum_{i=1}^{I2} P^*_{i,t-1}$ is the sum of the output of $I2$ shutdown units that need to be absorbed during the period $t-1$ to the period T. This will be 0 if there is no new shutdown unit in the current period. $\sum_{i=1}^{I} P_{i,t-1} - P_t$ is the load transfer value between time periods, that is, the difference between the sum of the actual group output of the last stage machine and the current given demand load P_t. $P^{on}_{i,t}$ is the corresponding output of the Ith unit in Z_{ti} and Z_{t-1}, and I_{on} is the number of I_{on} units in both combinations.

ΔP is updated to ΔP_{update} when I_{on}>1 to further limit the output range constraint.

$$\begin{cases} \Delta P_{update} = \Delta P - \sum_{i=1}^{I_{on}} (P^{on}_{i,t} - P^{on}_{i,t-1}), \sum_{i=1}^{I} P_{i,t-1} < P_t \\ \Delta P_{update} = \Delta P - \sum_{i=1}^{I_{on}} (P^{on}_{i,t-1} - P^{on}_{i,t}), \sum_{i=1}^{I} P_{i,t-1} > P_t \end{cases} \tag{11}$$

(2) If Z_{ti} = Z_{t-1}, that is, when the unit combination does not change in the current period, the load fluctuation is equally distributed to the running units.

$$\Delta P = \frac{\sum_{i=1}^{I} P_{i,t-1} - P_t}{n_{on}} \tag{12}$$

2.3. Fluctuation Evaluation Index

It is necessary to judge the stability of the overall change curve using qualitative analysis indicators to address the instability of and fluctuation in the load change in the unit output [20]. Therefore, the output curve of each unit in the operation cycle was evaluated using three indicators.

The average fluctuation amplitude was used to characterize the change and fluctuation in the continuous curve in adjacent periods [21]. The degree of fluctuation in the curve is proportional to the numerical value, reflecting the discrete degree of continuous data to a certain extent.

$$S^{\ i}_{AVR} = \frac{1}{T} \sum_{t=1}^{T-1} \left(\frac{P_{i,t+1} - P_{i,t}}{P_{i,max}} \times 100\% \right) \tag{13}$$

The power distribution skewness is an effective index of the fluctuation and inclination degree of the output curve of the reaction unit, and its value is directly proportional to the degree of the curve fluctuation [22].

$$S_P^{\ i} = \frac{1}{T} \sum_{t=1}^{T} \left(\frac{P_{i,t} - \overline{P_i}}{S^{\ i}_{SD}} \right)^3 \tag{14}$$

$$S_{SD}^{i} = \sqrt{\frac{\sum_{t=1}^{T}\left(P_{i,t} - \overline{P_i}\right)^2}{T}} \tag{15}$$

The output fluctuation ratio takes the average value of the unit output fluctuation in the load distribution period as the index to characterize the fluctuation trend.

$$S_{epsilon}^{\ i} = \frac{\sum_{t=1}^{T}\left|P_{i,t} - \overline{P_i}\right|}{\sum_{t=1}^{T} P_{i,t}} \times 100\% \tag{16}$$

where $\overline{P_i}$ is the average output of the i-th unit during the load distribution and S_{SD}^{i} is the standard deviation of the i-th unit.

3. Improved Biogeography-Based Optimization Algorithm

3.1. BBO Algorithm

The BBO aims to find the optimal solution by simulating the migration and emigration of adjacent individuals in the process of evolution and combining the mutation of these individuals. The fitness index of habitats is calculated before and after each migration to evaluate the quality of candidate solutions for waiting problems and compare individuals and habitats. Note that the species migration model and species migration operator are two important factors in the migration process. In addition, the fitness index of the habitat can be obtained by calculating the immigration probability and emigration probability of each individual, and the information between habitats can be transferred to improve the fitness of the entire solution group. Moreover, the fitness index is proportional to the quality of the candidate solutions.

The traditional migration model expressed in Equations (17) and (18) represents the evolution process of the i-th individual species with the number of species n; λ_{max} and μ_{max} are the maximum immigration rate and the maximum emigration rate, respectively, and λ and μ are the immigration and emigration probabilities, respectively. However, the oversimplified curve of species migration cannot simulate biological migration with high accuracy, because of which the model cannot meet the new requirements.

$$\lambda_i = \lambda_{max}\left(1 - \frac{i}{n}\right) \tag{17}$$

$$\mu_i = \frac{\mu_{max} i}{n} \tag{18}$$

In the BBO algorithm [23,24], a single individual can be considered as a habitat, and a habitat has a high habitat suitability index (HSI) if it is suitable for living organisms, and the influence factor related to HSI is the suitability index variables (SIVs). The HSI values between different habitats are exchanged through migration activities, which help to improve the overall fitness of the candidate solution set. Equation (19) then represents the species migration activity between habitats HSI_j and HSI_i. $\Omega(\lambda, \mu)$ is the migration operator, which adjusts the habitats through the migration probability λ and the emigration probability μ.

$$\Omega(\lambda, \mu) : HSI_i(f_{SIV}) \leftarrow HSI_j(f_{SIV}) \tag{19}$$

3.2. Improvement of BBO Algorithm

3.2.1. Improvement of the Migration Model

Ma et al. [25,26] have studied the influence of different migration function models on migration results, in which a sinusoidal function has better performance in simulating real evolution, and two-stage species migration models with different fitness were proposed. Therefore, in this study, we compared the relationship between the individual fitness and the average fitness of the population to replace migration models. At the beginning of population reproduction, species often have a higher immigration rate and lower emigration rate.

At the beginning of population reproduction, habitats tend to have a higher population migration rate and lower population migration rate. With the increase in species number, the migration rate of species in a habitat becomes lower and the migration rate becomes higher [14]. Meanwhile, with the increasing number of species, the habitat environment becomes worse, the migration rate of species is lower, and the migration rate is higher. The habitat has low adaptability and should be moved out when the individual habitat fitness index is lower than the group average fitness index. On the other hand, when the individual index is higher than the group average fitness index, the emigration function is dynamically adjusted, and the appropriate emigration rate is independently selected using Equations (20) and (21).

$$\lambda_i = \frac{\lambda_{max}}{2}\left(sin\left(\frac{\pi}{2} + \frac{i\pi}{n}\right) + 1\right) \tag{20}$$

$$\mu_i = \begin{cases} \frac{\mu_{max}}{2}, F(i) < F_average \\ \frac{\mu_{max}}{2}\left(-sin\left(\frac{\pi}{2} + \frac{i\pi}{n}\right) + 1\right), F(i) \geq F_average \end{cases} \tag{21}$$

Here, $F(i)$ is the fitness of the i-th individual and $F_average$ is the average fitness of the contemporary population.

3.2.2. Improvement of the Migration Operator

With the hybrid cross-mutation operation in the genetic algorithm, the traditional operator can be replaced by a hybrid migration operator [14], as shown in Equation (22). However, in this formula, r is a random parameter, which has certain randomness and cannot properly reflect the law of species migration and change. Therefore, the migration function in Equation (23) is used to realize the dynamic replacement of hybrid factors, and the habitat information and feature fusion in the migration process are dynamically adjusted by combining the habitat adjustment process with the actual migration probability. This avoids the simple substitution of the migration operator and the randomness of the random number r and synthesizes the change in the habitat fitness, which is conducive to expanding the search range of the optimal solution, enhancing the candidate set, and avoiding falling into a locally optimal solution. The traditional migration operator in the BBO algorithm can be replaced by a hybrid migration operator by combining the hybrid cross-variance operation in the genetic algorithm [14]; see Equation (22). The parameter r in Equation (22) satisfies a uniform distribution in the interval [0, 1], and the hybrid cross-variance operation allows the SIV in habitat HSI_i in Equation (22) to no longer simply be replaced by the SIV in habitat HSI_j, but to take a co-mixing approach, ensuring that habitats with high solution set quality are not weakened in the species migration process, while also allowing habitats with lower solution set quality to share SIVs with those of higher solution set quality during the migration operation, improving the overall quality of the solution set. However, r is a random parameter with some randomness. When the value of r is high, it makes habitats with high HSI values participate less in the migration process, but instead increases the influence of habitats with low HSI values in the migration process, which does not well reflect the pattern of species migration changes. In this paper, the migration operator in Equation (23) is used to achieve dynamic replacement of the mixing parameters. When the HSI value of HSI_j is higher than that of HSI_i, the migration probability μ_j of habitat HSI_j and the migration probability λ_i of habitat HSI_i are both lower, and $(1 - \mu_j)HSI_j(f_{SIV})$ is greater than $\lambda_i HSI_i(f_{SIV})$ according to Equation (23); the same is true when the HSI value of HSI_j is lower than that of HSI_i. Therefore, Equation (23) can effectively increase the influence and participation of habitats with high HSI values in the migration process, avoiding the simple substitution of the migration operator and the larger randomness of the random number r. It better integrates the change in habitat fitness, which is conducive to expanding the search range of the optimal solution and achieving the purpose of enhancing the candidate set and avoiding getting trapped in a local optimal solution.

$$\Omega^*(\lambda,\mu): HSI_i(f_{SIV}) \leftarrow rHSI_i(f_{SIV}) + (1-r)HSI_j(f_{SIV}), \tag{22}$$

$$\Omega^*(\lambda,\mu): HSI_i(f_{SIV}) \leftarrow \lambda_i HSI_i(f_{SIV}) + \left(1-\mu_j\right)HSI_j(f_{SIV}), \tag{23}$$

4. Double-Layer Nested Model Solving Process

In this study, the IBBO and DP models are nested to form a double-layer intelligent algorithm system, in which the IBBO model is the inner layer and the DP model is the outer layer. The DP model is used to optimize the unit commitment under constraints and obtain the candidate combination solution set (regarded as the most promising region). Furthermore, the inner-layer IBBO model is used to calculate the output distribution of the combinations in the candidate solution set using Equations (1) and (2) as the objective functions. Simultaneously, the optimal load distribution is carried out in combination with the output fluctuation constraint to limit the output fluctuation degree in the load distribution process, and the optimal solution is ultimately obtained. The specific steps are as follows:

(1) Combination screening of the outer layers. There are 2^n combination schemes for n hydraulic units, excluding those units that do not conform to Equations (3)–(7), and the remaining units are reserved as the input of the inner model of the candidate combination solution set.

(2) Calculation of the inner-layer output distribution. The output calculation is carried out for each combination in the combination candidate set. First, the population initialization is performed. Based on Equations (8)–(12), in the population initialization stage, the generation space of the solution is reduced using Equations (9) and (10) to limit the excessive increase or decrease in the unit output when the demand load changes. Then, the individual habitat suitability index is evaluated. Moreover, the migration model and migration operator expressed in Equations (20)–(23) are used to transfer and exchange information for individuals to expand the search range of the solution space, re-rank the habitats after information exchange, and obtain the optimal solution of the unit commitment output under the current iteration based on the maximum fitness.

(3) Obtaining the output distribution results corresponding to each combination in the candidate set of unit combinations at the end of the algorithm. It is necessary to comprehensively consider the vibration zone crossing coefficient, the extra startup/shutdown times of the unit, and the water consumption of the unit to select the optimal solution in the candidate set. The optimal unit combination and output of the corresponding unit in the current period can be obtained.

(4) Recording of the unit combination allocation information and related running time for completing the output allocation in the current period. Proceed to step (5) if $t \geq 96$ is reached, otherwise return to step (1).

(5) Analysis of the process data, including the flow rate and water consumption of the entire process, and ending the optimization of the operation strategy as a whole.

The load distribution time by time is optimized by using the double-layer nested model. The calculation flowchart of the model is shown in Figure 1.

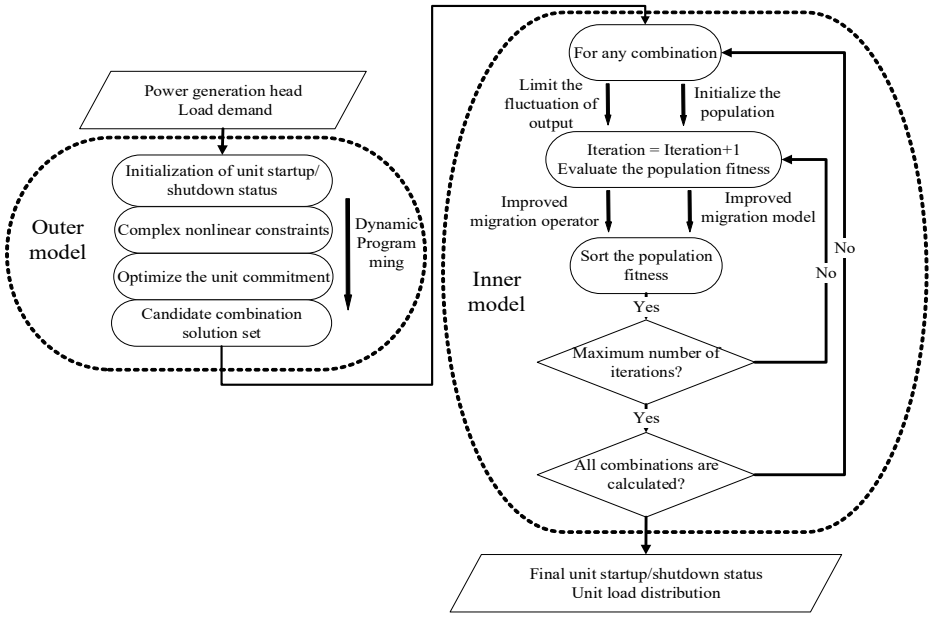


Figure 1. Calculation flowchart of the model.

5. Case Study

5.1. Ertan Hydropower Station

Ertan Hydropower Station is located at the junction of Yanbian and Miyi counties in Panzhihua City, the southwestern border of Sichuan Province, China, at the downstream end of the Yalong River, the largest tributary of the Jinsha River, as shown in Figure 2 [27]. Ertan Hydropower Station is the first power station in the three-stage development of the Yalong River Hydropower Base, which has the Guandi Hydropower Station and the Tongzilin Hydropower Station upstream and downstream, respectively. The total installed capacity of Ertan Hydropower Station is 3300 MW, consisting of six units of the same type, with a guaranteed output of up to 1000 MW and a multiyear average power generation capacity of 17 billion kW·h. The rated capacity and maximum output of each unit of Ertan Hydropower Station is 550 MW, the minimum output is 20 MW, and the minimum and maximum operating units are 2 and 6, respectively.

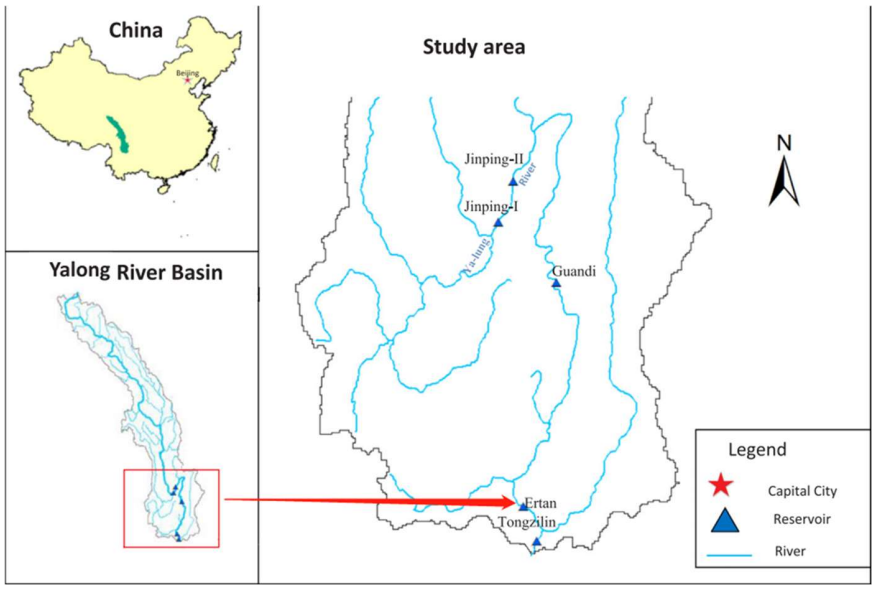


Figure 2. Location of Ertan Hydropower Station.

The data for this case study were selected from 15 min steps of power station demand load variation and generation head variation data for a single day in mid-March 2020 at Ertan Hydropower Station, as shown in Figure 3. The relevant parameters of Ertan Hydropower Station are shown in Table 1.

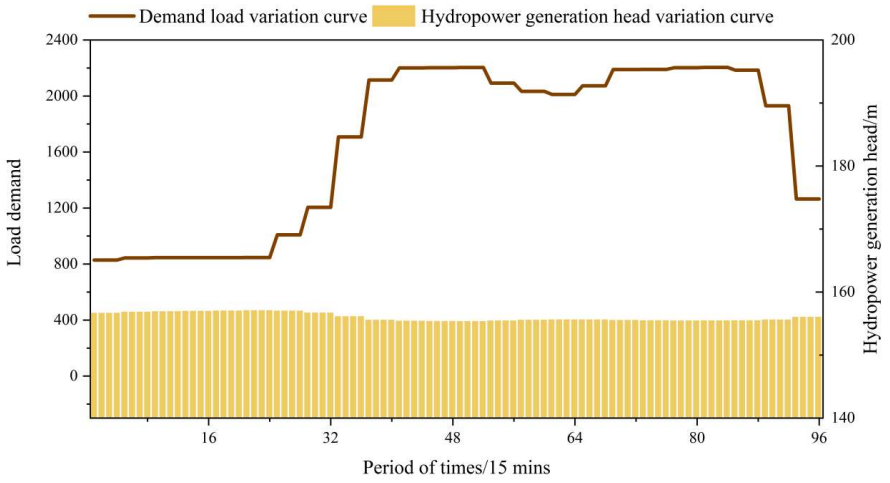


Figure 3. Ertan Hydropower Station demand load and generation head variation curve.

Table 1. Relevant parameters of Ertan Hydropower Station.

Parameters	Values	Units	Parameters	Values	Units
Normal storage level/maximum water level	1200	m	Unit vibration zone	[0, 20] ∪ [160, 430]	MW
Dead level/minimum water level	1150	m	Minimum operating/shutdown time	1	h
Maximum power generation head	186	m	Total storage capacity	5.8	km3
Minimum power generation head	135	m	Regulating reservoir capacity	3.37	km3

5.2. Case Analysis and Discussion

In order to verify the performance of the IBBO algorithm obtained by making improvements to the migration model and migration operator in this paper, a load period with a step length of 15 min was randomly selected from the selected computational data. On the MATLAB R2022b platform, the IBBO method proposed in this paper was compared with the IBBO algorithm proposed in reference [14] and converged with the traditional BBO algorithm, and they were set into three groups, A, B, and C, respectively. Based on past experience, the total number of iterations for the three algorithms was set to 300 and the population size was set to 50, and the rest of the relevant parameters were consistent with those of the reference [14]. The comparison of algorithm convergence curves is shown in Figure 4.

As can be seen from Figure 4, the overall convergence performance of Algorithm A is the best, and the curve converges to 1304.61 m^3/s at 50 iterations, which is 3.87% and 5.78% less than that of Algorithms B and C, respectively. Therefore, this shows that the convergence performance of Group A has been effectively improved by improving the migration model and operator, and the solution quality is better than that of the traditional BBO algorithm.

The IBBO-DP model and conventional dual dynamic programming (DDP) were used to calculate the load allocation of hydro units for the selected Ertan power plant demand load and generation head data, the unit crossing vibration zone constraint and unit output fluctuation constraint were not considered in the DDP model, and finally the load allocation results of the two models were compared with the actual operation results, as shown in

Table 2. It can be seen that the IBBO-DP model consumes the least amount of water in load distribution, saving 0.672% and 3.900% in water consumption compared with the DDP and actual operation results; the unit operates with the highest safety, achieving zero crossing of the unit's vibration zone, avoiding 30 and 12 nonessential vibration zone crossings compared with the DDP and actual operation results, respectively.

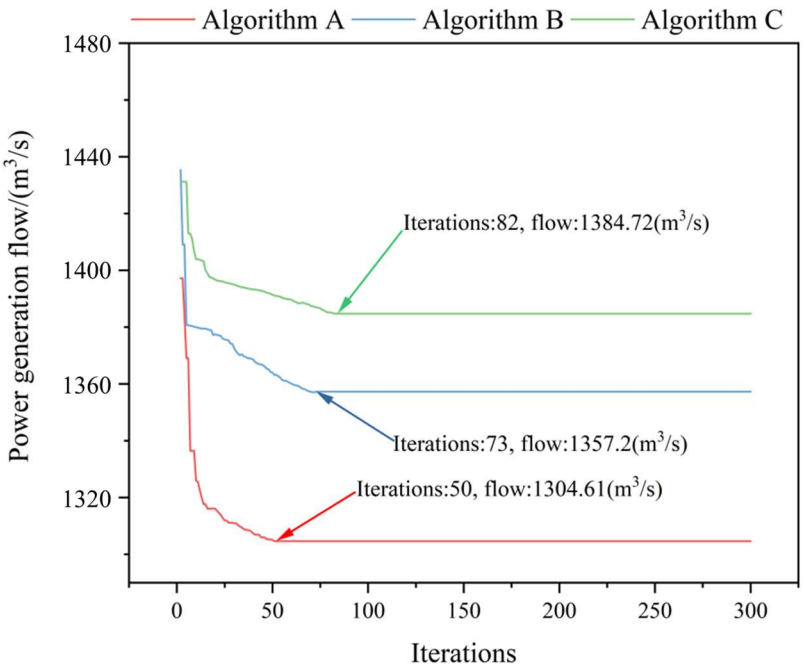


Figure 4. Model convergence curves for different BBO algorithms.

Table 2. Comparison of load distribution results.

	IBBO-DP	DDP	Actual Operation
Total water consumption/m^3	1.034×10^8	1.076×10^8	1.041×10^8
Average water consumption rate/(m^3/kW·h)	2.581	2.685	2.597
Additional startup and shutdown times/times	0	0	0
Times crossing vibration zone/times	0	30	12

Figure 5 shows the hourly generation savings of IBBO-DP compared with DDP during the load distribution process. As the demand load of Ertan Hydropower Station gradually increases, the percentage of generation flow saved by IBBO-DP gradually increases, with an average of 3.161% of generation flow saved per hour during the load distribution process, which is about 40.236% m^3/s. The maximum value is at the 9th hour of load distribution, and can save 3.864% of generation flow during the load distribution process. This shows that IBBO-DP has a more powerful optimization capability and can optimize the target function to a higher degree than DDP, and can optimize the generation flow rate on the basis of meeting the generation load demand of the power station.

Figure 6 shows the load distribution results for IBBO-DP and DDP. In the first third of the load distribution process, the results of the two models are relatively similar, with all three units sharing the power generation task, and the output change process is relatively smooth; however, as the demand load of the power station increases, each unit in DDP shows frequent fluctuations during the time period of 8 to 22 h, and the number of vibration zone crossings increases, which increases the safety risk of unit operation, while IBBO-DP has a more stable output process than DDP during this time period. When the demand load

changes frequently, the output values of each unit are reasonably matched, and the output change process and trend of each unit are relatively consistent, without large-amplitude and high-frequency output fluctuations.

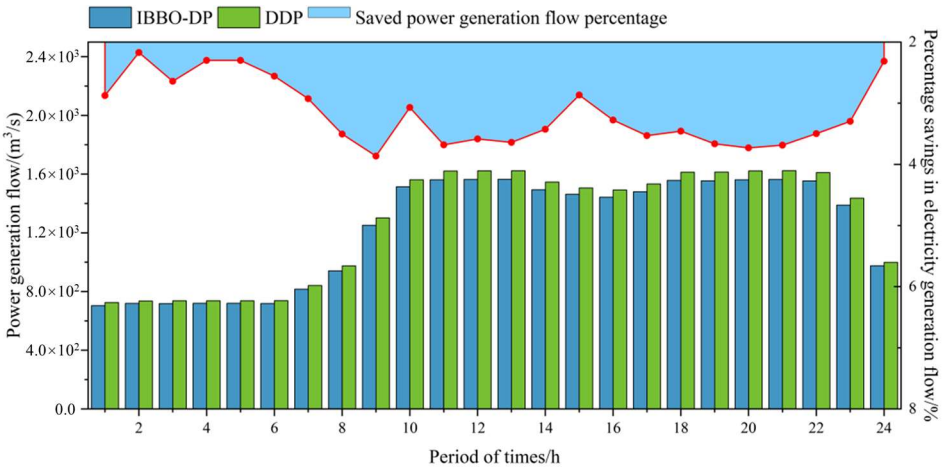


Figure 5. Comparison of generation flows for different models.

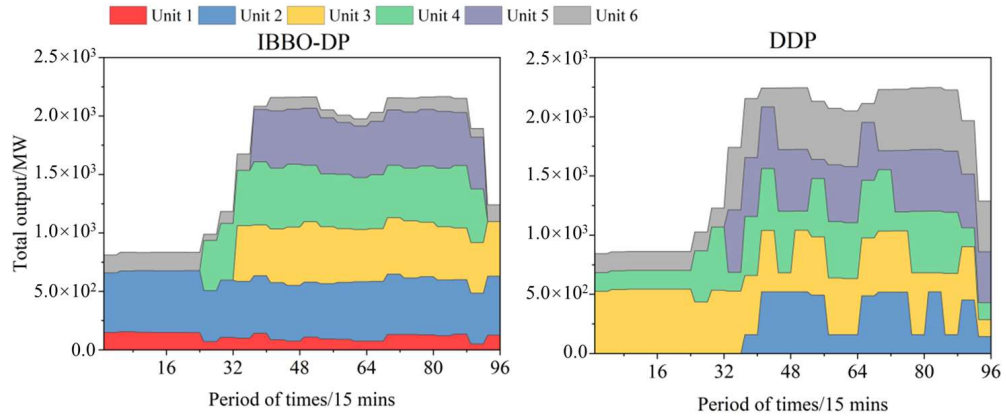


Figure 6. Comparison of load distribution results for different models.

For further analysis of the change in output power fluctuation and vibration zone crossing of each unit during load distribution, Table 3 shows the results of the unit fluctuation evaluation index for each unit of the different models during the load distribution process. (Because the power distribution skewness index S_P has positive and negative points, if the weighted averaging is performed directly, the fluctuations between the data are eliminated and no correct comparison can be made, so the average value of the units is not set for comparison.) Figure 7 shows the power output change curve of each unit of the different models during the load distribution process. As the No. 1 unit in DDP does not participate in the load distribution process, Figure 7 only shows the comparison of the output of the last five units. From Table 3 and Figure 7, it can be seen that IBBO-DP can effectively avoid the fluctuations in unit output due to changes in demand load. When comparing the average values of fluctuation indicators between the two models, IBBO-DP optimizes the average fluctuation amplitude of units to the highest extent, up to 45.53%, indicating that IBBO-DP can effectively limit the dispersion of the continuous output curves of each unit.

Table 3. Comparison results of average fluctuation ranges of six units.

Index		SAVR/%	SP	Sepsilon/%
Unit 1	IBBO-DP	3.59	−0.37	23.62
	DDP	0	0	0
Unit 2	IBBO-DP	0.82	−0.53	4.26
	DDP	5.59	0.31	90.68
Unit 3	IBBO-DP	1.53	−0.68	66.67
	DDP	4.20	−2.04	17.56
Unit 4	IBBO-DP	2.62	−0.86	58.33
	DDP	5.67	−0.13	49.46
Unit 5	IBBO-DP	2.11	−0.32	83.33
	DDP	3.94	−0.39	74.57
Unit 6	IBBO-DP	4.44	−0.32	29.34
	DDP	3.65	−0.28	46.06
Average	IBBO-DP	2.51		44.25
	DDP	4.61		55.66

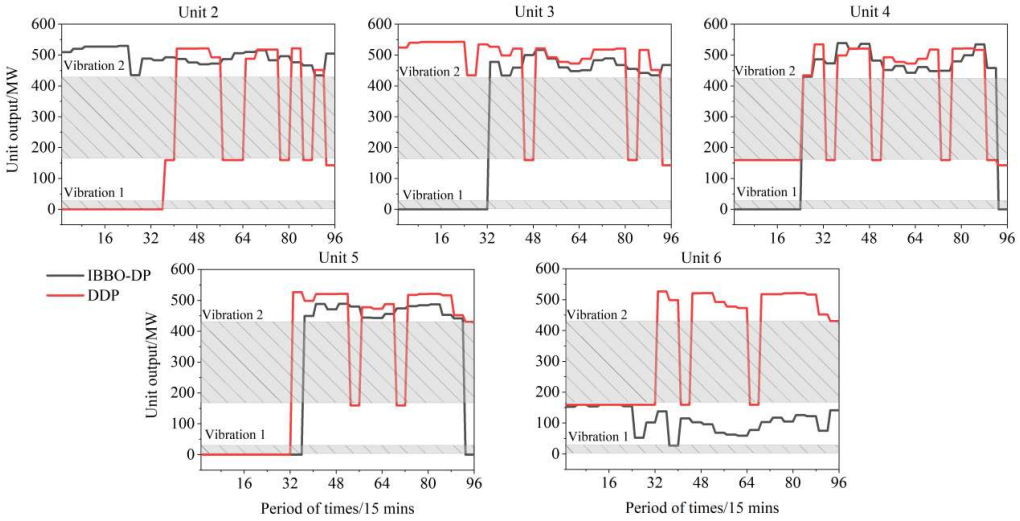


Figure 7. Variation curves of the output of each unit for different models.

In terms of the degree of optimization of the indicators, the most obvious degree of optimization is found in IBBO-DP's Unit 2, where the output range is concentrated within [460, 530] MW, with the S_{AVR} being only 0.82%, and the fluctuation in output can be suppressed by 85.33% compared with DDP; the power distribution skewness S_P and fluctuation output ratio $S_{epsilon}$ are −0.53 and 4.26%, respectively, with the average fluctuation amplitude S_{AVR} and fluctuation output ratio $S_{epsilon}$ being the lowest among the six units. In terms of the fluctuating output ratio $S_{epsilon}$, it can be found that Units 3, 4, and 5 under IBBO-DP are higher than DDP, with Unit 3 being the most obvious, with a 73.77% higher fluctuating output ratio $S_{epsilon}$ than DDP. Combined with the analysis in Figure 7, this is because Unit 3 under IBBO-DP is less involved in the load distribution process than under DDP, and the output range is concentrated within [430, 500] MW, while the fluctuating output ratio indicator aims to calculate the average fluctuating output of the unit compared with the total output of the unit in consecutive periods, so when the output of the unit is 0 for some periods, this easily leads to a higher average fluctuating output of the unit, thus making the fluctuating output ratio value of the unit relatively higher.

Figure 8 shows the comparison between the IBBO-DP model and the DDP model in terms of total water consumption and the number of unit vibration zone crossings during load distribution on the same day in the middle of each month in 2020, compared with the actual operating results of the plant on that day. Analysis of the water consumption comparison graphs on the left shows that IBBO-DP achieves different degrees of water

consumption optimization compared with DDP and actual plant operation, with average optimizations of 3.44% and 5.01%, respectively, which are significant degrees of optimization. Combined with the comparison of the number of vibration zone crossings on the right side of Figure 8, it can be found that IBBO-DP can avoid more unit vibration zone crossings in January, October, and December, and can optimize the number of unit vibration zone crossings in the load distribution process from 4 to 22 times compared with the actual operation of the power station, thus effectively reducing the unit vibration zone crossings. This results in a reduction in water consumption when crossing the vibrating zone and thus further savings in water consumption.

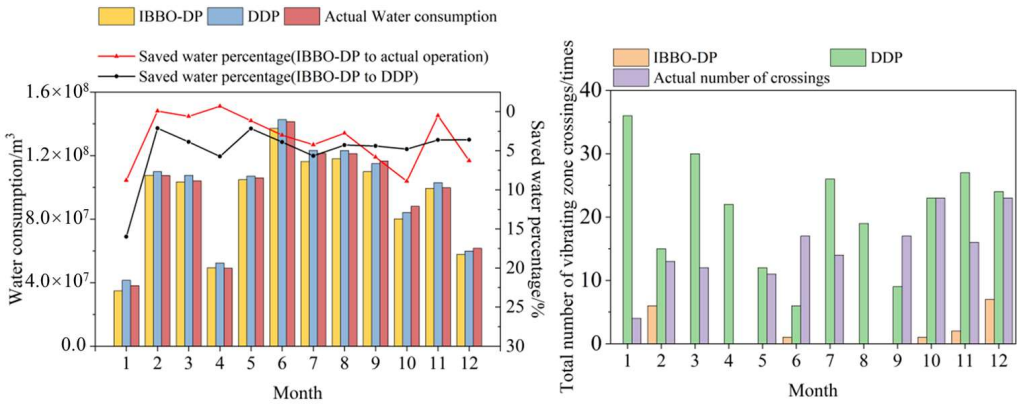


Figure 8. Comparison of the degree of optimization of water consumption and the number of times the unit crosses the vibration zone in different months.

6. Conclusions

In this study, an IBBO-DP two-layer nested model was constructed. The outer layer is the DP model, which is responsible for the optimization of unit commitment under multiple constraints. The inner layer is based on an improved biogeography-based optimization algorithm, which proposes a unit output fluctuation constraint, with the optimal output of the previous unit and the unit combination change as the judgment conditions, and constructs a unit load allocation optimization model. Based on a practical case with a minimum step of 15 min, this study uses the IBBO-DP model hydro unit load allocation for optimization and compares the results with the DDP model and the actual operation results. From the results of this study, the following conclusions can be drawn:

(1) By improving the BBO algorithm and establishing the dynamic migration model based on the group average adaptation degree and the adaptive migration operator with the hybrid crossover idea, the convergence ability and the merit-seeking ability of the BBO algorithm can be further improved.

(2) In actual operation, the IBBO-DP model can better match the number of units and the corresponding unit load during the peak load period and the period of frequent load changes, preventing the units from crossing the vibration zone frequently, reducing the water consumption by 0.672% and 3.900%, and reducing the number of vibration zone crossings by 30 and 20 times, respectively, compared with the DDP model and the actual operation of the power plant, and taking more comprehensive consideration of economy and safety in the process of load distribution. More comprehensive consideration of economy and safety is more in line with the actual operation of the hydropower unit.

(3) Considering the constraint of unit output fluctuation, the IBBO-DP model can effectively suppress and weaken the unit output fluctuation and unstable operation caused by the change in demand load and unit combination in the hydropower unit load allocation process, and the average reduction in the fluctuation evaluation index can reach 52.91%.

These conclusions verify that the double-layer nested model can optimize the load distribution of hydropower units to a certain extent, and the load distribution optimization

of hydropower units under the complementary mode of water and light can be studied on this basis. Although the model constructed in this study allows the unit to avoid crossing the vibration zone during operation, there is a risk of insufficient or loss of unit output. In subsequent research, further consideration will be given to the constraint of the unit output slope ratio when distributing the load of hydroelectric units. In addition, more operating data from power plants will be collected for research to improve the reliability of the model.

Author Contributions: Conceptualization, H.P. and Y.Z.; methodology, H.P. and Z.L.; software, Z.L.; validation, C.H. and F.F.; data curation, X.Z.; writing—original draft preparation, Z.L.; writing—review and editing, C.H. and H.P.; supervision, Y.Z. All authors have read and agreed to the published version of the manuscript.

Funding: This work was supported by the State Key Program of the National Natural Science Foundation of China (52339006).

Data Availability Statement: The data will be made available by the authors on request.

Acknowledgments: The authors appreciate the High-Performance Computing of Hohai University.

Conflicts of Interest: Zhengliang Luo was employed by Ming Yang Smart Energy Group Limited. The remaining authors declare that the research was conducted in the absence of any commercial or financial relationships that could be construed as a potential conflict of interest. Ming Yang Smart Energy Group Limited had no role in the design of the study; in the collection, analyses, or interpretation of data; in the writing of the manuscript, or in the decision to publish the results.

Nomenclature

W	The minimum water consumption
I	The number of units
T	The number of periods
$Q_{i,t}(H_t, P_{i,t})$	The flow consumption of the i-th unit in period t
Δt	The time granularity
$\lambda_{i,t}$	The startup/shutdown state of the i-th unit in period t
n_{cross}	The number of times the unit crosses the vibration zone
W_{on_off}, W_{cross}	The extra startup and shutdown times (excluding the initial startup/shutdown and the last stop) of the unit
$P_{i,t}$	The output of the i-th unit
P_{dt}	The demand load of the power grid during period t
θ_t	The percentage deviation between the sum of the output of each unit and the demand load of the power grid during period t
$\overline{P_{i,t}}, \underline{P_{i,t}}$	The upper and lower limits of the vibration zone
$T_i^{on}, \overline{T_i^{off}}$	The continuous starting and stopping times of the i-th unit
$T_{min}^{on}, T_{min}^{off}$	The minimum limit time for starting and stopping the i-th station
$N_{i,t}^{on,off}$	The extra startup/shutdown times of the ith unit at moment t
$N_{max}^{on,off}$	The sum of the maximum allowable startup/shutdown times of all units in the entire dispatching process
δ	The deviation of the power grid demand load
V_t	The storage capacity of the power station at time t
V^{min}, V^{max}	The minimum and maximum values of the storage capacity of the power station
Q_t^{in}, Q_t^{out}	The inlet flow and outlet flow of the power station at time t
Wq_{t-1}	The disposal volume of the power station at time $t-1$
$Z_{t1}, Z_{t2}, \ldots, Z_{tn}$	The N unit combinations in period T ($t > 1$)
Z_{t-1}	The corresponding combination of optimal load distribution in period $t-1$
$\Delta P, \Delta P_{update}$	The unit output fluctuation range constraint before and after the update
$P_{i,t}^*$	The output of the newly started unit
$P_{i,min}^n$, $P_{i,max}^n$	The minimum and maximum boundaries of the n-th operational zone of the i-th unit
$P_{i,t}^{on}$	The corresponding output of the Ith unit in Z_{ti} and Z_{t-1}

I_{on}	The number of units in both combinations
S_{AVR}^{i}	The average fluctuation amplitude of the i-th unit
S_{P}^{i}	The power distribution skewness of the i-th unit
S_{SD}^{i}	The standard deviation of the i-th unit
$S_{epsilon}^{i}$	The output fluctuation ratio of the i-th unit
$\overline{P_i}$	The average output of the i-th unit during the load distribution
λ_{max}, μ_{max},n	The maximum migration probability, maximum migration probability, and species number
λ_i, μ_i	The migration probability and migration probability of the i-th habitat
HSI_i	The habitat suitability index of the i-th habitat
f_{SIV}	The suitability index variables
$\Omega(\lambda, \mu)$	The migration operator

References

1. Gao, Y.; Xu, W.; Wang, Y.; Wen, X. Study on Internal Economic Operation of Large Hydropower Station Based on Load Optimal Distribution Table. *Water Resour. Power* **2023**, *41*, 197–201.
2. Cheng, Q.; Ming, B.; Liu, P.; Huang, K.; Gong, Y.; Li, X.; Zheng, Y. Solving hydro unit commitment problems with multiple hydraulic heads based on a two-layer nested optimization method. *Renew. Energy* **2021**, *172*, 317–326. [CrossRef]
3. Wang, H.; Ma, M. Regulation Characteristics and Load Optimization of Pump-Turbine in Variable-Speed Operation. *Energies* **2021**, *14*, 8484. [CrossRef]
4. Han, S.; Yuan, Y.; He, M.; Zhao, Z.; Xu, B.; Chen, D.; Jurasz, J. A novel day-ahead scheduling model to unlock hydropower flexibility limited by vibration zones in hydropower-variable renewable energy hybrid system. *Appl. Energy* **2024**, *356*, 122379. [CrossRef]
5. Lu, L.; Yuan, W.; Su, C.; Wang, P.; Cheng, C.; Yan, D.; Wu, Z. Optimization model for the short-term joint operation of a grid-connected wind-photovoltaic-hydro hybrid energy system with cascade hydropower plants. *Energy Convers. Manag.* **2021**, *236*, 114055. [CrossRef]
6. Levieux, L.I.; Inthamoussou, F.A.; De Battista, H. Power dispatch assessment of a wind farm and a hydropower plant: A case study in Argentina. *Energy Convers. Manag.* **2019**, *180*, 391–400. [CrossRef]
7. Zhai, Q.; Zhou, Y.; Li, X.; Wu, J.; Xu, Z.; Xie, X. Unpredictability and full scenario feasibility: Current situation, challenges and future of dealing with load and renewable energy uncertainty. *Proc. CSEE* **2020**, *40*, 6418–6433.
8. Yan, S.; Chen, F.; Yang, J.; Zhao, Z. A Multistep Prediction Model for the Vibration Trends of Hydroelectric Generator Units Based on Variational Mode Decomposition and Stochastic Configuration Networks. *Sensors* **2023**, *23*, 9762. [CrossRef]
9. Yang, X.; Fan, X.; Chen, Q. Control Strategy of Hydropower Plant Considering Vibration Region and Its Application in Coordinated Hydro and Wind Power Generation. *Proc. CSEE* **2019**, *39*, 5433–5441+5591.
10. Wang, A.; Hu, S. Real-time economic and safe operation diagnosis of hydropower units. *J. Phys. Conf. Ser.* **2023**, *2564*, 12059. [CrossRef]
11. Cheng, C.; Zhao, Z.; Jin, X.; Liu, L.; Zhong, R. Automatic avoidance method of irregular multi-restricted areas for large units with high water head in cascade hydropower stations. *J. Hydraul. Eng.* **2019**, *50*, 1299–1310.
12. Zhao, Z.; Cheng, C.; Liao, S.; Li, Y.; Lu, Q. A MILP Based Framework for the Hydro Unit Commitment Considering Irregular Forbidden Zone Related Constraints. *IEEE Trans. Power Syst* **2020**, *36*, 1819–1832. [CrossRef]
13. Liao, S.; Liu, Z.; Liu, B.; Wu, X.; Cheng, C.; Su, H. Short-Term Hydro Scheduling Considering Multiple Units Sharing a Common Tunnel and Crossing Vibration Zones Constraints. *J. Water Resour. Plan. Manag.* **2021**, *147*, 04024063. [CrossRef]
14. Chen, D.; Gong, Q.; Qiao, H.; Zhao, J. Multi-objective generation scheduling of wind power grid-connected power system using improved biogeography algorithm. *Proc. CSEE* **2012**, *32*, 150–158+231.
15. Li, B.; Deng, H.; Wang, J. Optimal Scheduling of Microgrid Considering the Interruptible Load Shifting Based on Improved Biogeography-Based Optimization Algorithm. *Symmetry* **2021**, *13*, 1707. [CrossRef]
16. Liu, F.; Gu, B.; Qin, S.; Zhang, K.; Cui, L.; Xie, G. Power grid partition with improved biogeography-based optimization algorithm. *Sustain. Energy Technol. Assess.* **2021**, *46*, 101267. [CrossRef]
17. Pei, P.; Li, C.; Lu, B. BBO algorithm with improved migration operator and its optimization in PID parameters. *Comput. Appl.* **2020**, *40*, 728–734.
18. Garg, V.; Deep, K.; Padhee, N. Constrained Laplacian Biogeography-Based Optimization for Economic Load Dispatch Problems. *Process Integr. Optim. Sustain.* **2022**, *6*, 483–496. [CrossRef]
19. Yu, Y.; Wu, Y.; Liu, X. Study on the economic load distribution strategy of hydropower station AGC considering the risk of unit crossing vibration zone. *Power Grid Technol.* **2020**, *44*, 2673–2682.
20. Wang, X.; Mei, Y.; Cai, H.; Cong, X. A new fluctuation index: Characteristics and application to hydro-wind systems. *Energies* **2016**, *9*, 114. [CrossRef]
21. Zhu, Y.; Huang, W.; Chen, S.; Ma, G.; Han, X. Intraday optimal operation strategy of water and light complementation. *Adv. Eng. Sci.* **2021**, *53*, 142–149.

22. Zhu, Y.; Chen, S.; Ma, G.; Han, X.; Wang, L. Short-term dispatch of hydropower and light complementation considering fluctuation of power generation and output. *J. Electrotech. Technol.* **2020**, *35*, 2769–2779.
23. Simon, D. Biogeography-based optimization. *IEEE Trans. Evol. Comput.* **2008**, *12*, 702–713. [CrossRef]
24. Aggarwal, S.K.; Saini, L.M.; Sood, V. Large Wind Farm Layout Optimization Using Nature Inspired Meta-heuristic Algorithms. *IETE J. Res.* **2023**, *69*, 2683–2700. [CrossRef]
25. Ma, H. An analysis of the equilibrium of migration models for biogeography-based optimization. *Inf. Sci.* **2010**, *180*, 3444–3464. [CrossRef]
26. Zhao, F.; Qin, S.; Zhang, Y.; Ma, W.; Zhang, C.; Song, H. A two-stage differential biogeography-based optimization algorithm and its performance analysis. *Expert Syst. Appl.* **2019**, *115*, 329–345. [CrossRef]
27. Tan, Q.; Wen, X.; Fang, G.; Wang, Y.-Q.; Qin, G.-H.; Li, H.-M. Long-term optimal operation of cascade hydropower stations based on the utility function of the carryover potential energy. *J. Hydrol.* **2020**, *580*, 124359. [CrossRef]

Disclaimer/Publisher's Note: The statements, opinions and data contained in all publications are solely those of the individual author(s) and contributor(s) and not of MDPI and/or the editor(s). MDPI and/or the editor(s) disclaim responsibility for any injury to people or property resulting from any ideas, methods, instructions or products referred to in the content.